Mechanical Systems and Signal Processing 130 (2019) 395–408

Contents lists available at ScienceDirect

Mechanical Systems and Signal Processing

journal homepage: www.elsevier.com/locate/ymssp

Identification of multiple leaks in pipeline III: Experimental results

Xun Wang *, Mohamed S. Ghidaoui, Jingrong Lin

Department of Civil and Environmental Engineering, Hong Kong University of Science and Technology, Clear Water Bay, Hong Kong, China

ARTICLE INFO

Article history:
Received 12 January 2019
Received in revised form 30 March 2019
Accepted 11 May 2019

Keywords:
Multi-leak identification
Transient waves
Maximum likelihood
Iterative beamforming
Akaike information criterion
Viscoelastic pipe

ABSTRACT

Identifying multiple leaks in a water supply pipe is challenging because pipe systems are complex and many parameters need to be estimated. In order to solve this problem, in Part I and Part II of the series of papers Wang and Ghidaoui (2018, 2019), a linearized model of transient wave in pipes was introduced, a maximum likelihood (ML) scheme to estimate leaks was proposed (for large leak number, the iterative beamforming method was used to simplify the ML solution), and the model selection methods were used to decide the leak number. In the present paper (Part III), these methods are experimentally justified via transient tests from a newly-built high-density polyethylene (HDPE) pipe system in the Water Resources Research Laboratory at the Hong Kong University of Science and Technology. Since the experiments are conducted in a viscoelastic pipe, the previous transient wave model (for elastic pipes) is modified to quantify the viscoelastic behavior of pipe wall. Experimental results with two and three leaks show that the proposed approaches are able to accurately localize the multiple leaks and decide the number of leaks.

1. Introduction

Leakage detection in water supply systems is an important societal problem. Transient-based detection methods (TBDMs) [1–18] have been widely-used which detect leaks by introducing hydraulic transient waves and analyzing their reflections [3,19–22], damping [6,23], or whole measured signals in either time or frequency domain [2,4,7–10,15,16,24–33].

While single-leak detection problem has been investigated more in depth, until recently few studies have carried out the problem of identifying multiple leaks systematically. The detectability of two leaks by means of TBDMs is pointed out on the basis of experimental results in [3]. Inverse transient analysis (ITA) method [2,4,31] assumes some discrete points in the pipe as potential leaks and estimates the corresponding leak sizes at these points by matching the time-domain numerical transient model and measured pressure [34]. However, ITA has to solve a high-dimensional optimization problem (the dimension equals to the assumed potential leak number). This means a high computational cost and, more importantly, a high computation complexity, which usually results in a wrong estimate of leaks due to local maximum traps. By investigating the pattern of peaks of frequency response function (FRF), multi-leak detection methods have been proposed in [8–10]. However, in real experiments, only a few FRF peaks can be observed due to limited valve closure speed, the damping of FRF increases exponentially with frequency, and the measurements are largely contaminated by noise. Therefore, the desired peak pattern of FRF usually cannot be observed such that these methods cannot be used.

* Corresponding author.
E-mail address: xunwang00@gmail.com (X. Wang).

https://doi.org/10.1016/j.ymssp.2019.05.015
0888-3270/

Nomenclature

q and h (transient) discharge and pressure head
$\mathbf{x}^L$ $(x^{L_n}, n = 1, \cdots, N)$ leak location
$\mathbf{s}^L$ $(s^{L_n}, n = 1, \cdots, N)$ leak size
x_m sensor coordinate
$\Delta\mathbf{h}$ head difference
$\mathbf{n}$ measurement noise
a wave speed
a_{ve} and a_e wave speed in viscoelastic and elastic pipes
g gravitational acceleration
A area of pipe
l pipe length
d internal pipe diameter
ω angular frequency
ω_{th} fundamental angular frequency
M sensor number
J frequency number
N leak number
$\log L$ log-likelihood function
$J_i, \tau_i, 1 = 1, \cdots, N_{kv}$ coefficients in the K-V model
N_{kv} order of the K-V model

Superscripts
U upstream
D downstream
L, L_n leak
M measurement
NL no leak
H conjugate transpose

Acronyms
AIC Akaike information criterion
FRF frequency response function
HDPE high-density polyethylene
IB iterative beamforming
K-V Kelvin-Voigt
MFP matched-field processing
ML maximum likelihood

Recently, [35] proposes a linear approximation model of wave propagation in a pipe with multiple leaks. Based on this linear model, a maximum likelihood (ML) multi-leak estimation method is proposed that estimates locations and sizes of multiple leaks separately and sequentially [35]. Furthermore, in order to cope with the computational complexity of the ML method in the case of large leak number, [36] uses an iterative scheme of ML, known as the iterative beamforming (IB) method [37–40], to simplify the optimization problem from N-dimensional (N is the assumed leak number) to one-dimensional. Furthermore, [36] also proposes to use the model selection methods, more specifically Akaike information criterion (AIC) [41] and Bayesian information criterion (BIC) [42], to decide the number of leaks existed in the pipe. The aforementioned methods have been justified via numerical simulation in [35,36].

The present paper verifies the multi-leak identification methods in [35,36] via experimental data obtained from a recently-built pipe system in the Water Resources Research Laboratory at the Hong Kong University of Science and Technology, where the pipe wall material is high-density polyethylene (HDPE). Therefore, the viscoelastic effect of pipe deformation during transient pressure behavior [13,43–50] is considered (the transient wave model in [35,36] is for elastic pipes). More specifically, the viscoelastic effect is modeled via the generalized Kelvin-Voigt (K-V) model. The resulting change is equivalent to an altered wave speed which becomes frequency-dependent [51]. As a result, the leakage detection methods in [35,36] can be applied.

The organization of this paper is as follows. Section 2 introduces the considered model of transient wave in viscoelastic pipes. Then, the strategy for multi-leak detection is summarized in Section 3. Section 4 shows the experimental results of identifying two leaks and three leaks. Finally, conclusions are drawn in Section 5.

2. Transient wave in a viscoelastic pipe

The pipeline configuration is illustrated in Fig. 1. The pipe length is l and internal cross-sectional diameter is d. The upstream and downstream ends of the single pipe locate at $x = x^U = 0$ and $x = x^D = l$, respectively. A valve is set at x^D to generate transient waves. It is assumed that N leaks exist in the pipe; their locations and sizes are denoted by x^{L_n} and s^{L_n} $(n = 1, \cdots, N)$, respectively.

The head difference due to leaks obtained from M sensors ($x_m, m = 1, \cdots, M$) and J frequencies ($\omega_j, j = 1, \cdots, J$) is used for leakage detection (in general, $M \ll J$), which approximately follows the linear model [35]:

$$\Delta\mathbf{h} \approx \mathbf{G}(\mathbf{x}^L)\mathbf{s}^L + \mathbf{n} = \sum_{n=1}^{N}\mathbf{G}_n(x^{L_n})s^{L_n} + \mathbf{n}. \tag{1}$$

In this equation, $\Delta\mathbf{h} = (\Delta h_{jm})_{m=1,j=1}^{MJ}$ is a MJ-dimensional vector in which $\Delta h_{jm} = h_{jm}^{M} - h_{jm}^{NL}$ denotes the head difference between the head measurement h_{jm}^{M} and theoretical head that does not include the leak terms

$$h_{jm}^{NL} = h^{NL}(x_m, \omega_j) = -Z(\omega_j)\sinh(\mu(\omega_j)x_m)q(x^U, \omega_j) + \cosh(\mu(\omega_j)x_m)h(x^U, \omega_j). \tag{2}$$

In Eq. (2), $Z(\omega) = \mu(\omega)a^2/(\mathrm{i}\omega gA)$ is the characteristic impedance, $\mu(\omega) = a^{-1}\sqrt{-\omega^2 + \mathrm{i}gA\omega R}$ is the propagation function, ω is angular frequency, a is the wave speed, g is the gravitational acceleration, A is the cross-sectional area of pipe, and R is the frictional resistance term. The matrix $\mathbf{G} = (\mathbf{G}_1, \cdots, \mathbf{G}_N)$ in Eq. (1) is an $MJ \times N$-dimensional matrix whose n-th column is an MJ-dimensional vector $\mathbf{G}_n(x^{L_n}) = (G(\omega_j, x^{L_n}, x_m))_{m=1,j=1}^{MJ}$, in which

$$G(\omega_j, x^{L_n}, x_m) = -\frac{\sqrt{g}Z(\omega_j)\sinh(\mu(\omega_j)(x_m - x^{L_n}))}{\sqrt{2\left(H_0^{L_n} - z^{L_n}\right)}}\left(Z(\omega_j)\sinh(\mu(\omega_j)x^{L_n})q(x^U, \omega_j) - \cosh(\mu(\omega_j)x^{L_n})h(x^U, \omega_j)\right), \tag{3}$$

where H^{L_n} and z^{L_n} are the steady-state pressure head and the pipe elevation at the leak x^{L_n}. Furthermore, $\mathbf{s}^L = (s^{L_1}, \cdots, s^{L_N})^\top$ and the MJ-dimensional vector $\mathbf{n} = (n_{mj})_{m=1,j=1}^{MJ}$ includes the random noise terms. Here, it is assumed that $\mathbf{n}$ follows independent and identically distributed (i.i.d.) Gaussian distribution with $\mathbf{0}$-mean and covariance matrix $\sigma^2\mathbf{I}$, where $\mathbf{I}$ is the identity matrix. The boundary conditions $h(x^U, \omega_j)$ and $q(x^U, \omega_j)$ in Eqs. (2) and (3) are given as follows. In the experiment considered in this paper, the pipe upstream is connected to a pump (introduced later in Section 4.1), thus $h(x^U, \omega_j) = 0$ is assumed. Furthermore, we measure pressure at x_0, which is close to x^U, and estimate the discharge at upstream $q(x^U, \omega_j)$ as [35,52,53]:

$$\hat{q}(x^U, \omega_j) = -\frac{h(x_0, \omega_j)}{Z(\omega_j)\sinh(\mu(\omega_j)(x_0 - x^U))}. \tag{4}$$

Note that if the pipe material is elastic [35,36], the wave speed is

$$a = a_e = \left(\rho\left(\frac{1}{\kappa} + (1 - \nu^2)\frac{d}{e}J_0\right)\right)^{-\frac{1}{2}}, \tag{5}$$

where κ and ρ are the bulk modulus and the density of the water, ν is the Poisson's ratio, e is the pipe wall thickness, $J_0 = 1/E$ where E is the Young's modulus of elasticity of pipe wall. In the case of viscoelastic pipe, the pipe wall deformation behavior can be equivalently quantified by modifying the wave speed (5) to

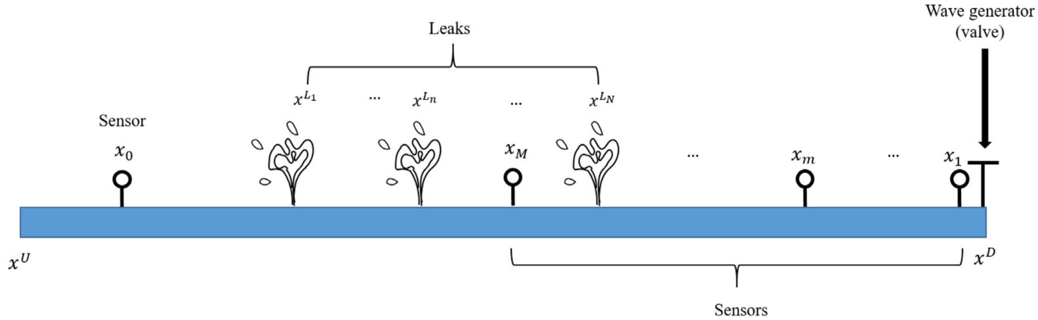

Fig. 1. Pipeline system with multiple leaks.

$$a = a_{ve}(\omega) = \left(\rho\left(\frac{1}{\kappa} + (1-\nu^2)\frac{d}{e}\left(J_0 + \sum_{i=1}^{N_{kv}} \frac{J_i}{1 + \mathrm{i}\omega\tau_i}\right)\right)\right)^{-\frac{1}{2}}. \tag{6}$$

Here, the wave speed becomes frequency-dependent because the retarded strain (time-dependent) is considered in the viscoelastic model. The details for deriving the equivalence of the viscoelasticity and the frequency-dependent wave speed can be found in [51]. It is assumed that viscoelastic pipe wall deformation during transient wave is modeled by the generalized K-V model [44] which appears in the summation term in Eq. (6): J_i and τ_i $(i = 1, \cdots, N_{kv})$ are the coefficients of the generalized K-V model and N_{kv} is the truncated order. These coefficients are calibrated via a transient test without leak prior to the leaking test. More specifically, they are estimated such that the transient wave model (without leak but J_i and τ_i are free parameters) is closest to the measured data. This method allows simulating properly the transient behavior of a pipe with leaks [54,55].

3. Strategy for estimating multiple leaks

This section summarizes the strategy to estimate the locations, sizes, and number of leaks in [35,36]. Given an assumed leak number N, the leaks are estimated by maximizing the log-likelihood function:

$$\log L(N, \mathbf{x}^L, \mathbf{s}^L | \Delta\mathbf{h}) = -JM\log(\pi\sigma^2) - \frac{\left\|\Delta\mathbf{h} - \mathbf{G}(\mathbf{x}^L)\mathbf{s}^L\right\|^2}{\sigma^2}. \tag{7}$$

with respect to $\mathbf{x}^L$ and $\mathbf{s}^L$. This leads to the estimates of locations and sizes of the N leaks:

$$\hat{\mathbf{x}}^L = \arg\max_{\mathbf{x}^L}\left(\Delta\mathbf{h}^H\mathbf{G}(\mathbf{x}^L)\left(\mathbf{G}^H(\mathbf{x}^L)\mathbf{G}(\mathbf{x}^L)\right)^{-1}\mathbf{G}^H(\mathbf{x}^L)\Delta\mathbf{h}\right) \tag{8}$$

and

$$\hat{\mathbf{s}}^L = \left(\mathbf{G}^H(\hat{\mathbf{x}}^L)\mathbf{G}(\hat{\mathbf{x}}^L)\right)^{-1}\mathbf{G}^H(\hat{\mathbf{x}}^L)\Delta\mathbf{h}. \tag{9}$$

In the case that assumed leak number $N = 1, 2$, the leak localization can be accomplished by directly plotting Eq. (8) and finding its maximum (when $N = 1$ the method is also known as matched-field processing in [32,51]). However, for a large N, exhaustively searching the maximum of Eq. (8) implies a high computational cost and directly solving the optimization problem Eq. (8) is troublesome due to the complexity of the objective function which has many local maxima. Therefore, for $N \geqslant 3$, an iterative version of the ML strategy based on the expectation-maximization (EM) algorithm [56,57], known as IB, is used. Here, the main steps of IB for leakage detection are listed; an introduction of IB with its principle and more details can be found in [36].

First, initial leak locations $\mathbf{x}_0^L = \left(x_0^{L_1}, \cdots, x_0^{L_N}\right)^\top$ and sizes $\mathbf{s}_0^L = \left(s_0^{L_1}, \cdots, s_0^{L_N}\right)^\top$ are given. Assume that $\mathbf{x}_{k-1}^L = \left(x_{k-1}^{L_1}, \cdots, x_{k-1}^{L_N}\right)^\top$ and $\mathbf{s}_{k-1}^L = \left(s_{k-1}^{L_1}, \cdots, s_{k-1}^{L_N}\right)^\top$ from $(k-1)$-th iteration are known, then the contributions from various leaks to the measurement $\Delta\mathbf{h}$ are estimated as

$$\hat{\mathbf{c}}_{nk} = \mathbf{G}_n(x_{k-1}^{L_n})s_{k-1}^{L_n} + \frac{1}{N}(\Delta\mathbf{h} - \mathbf{G}(\mathbf{x}_{k-1}^L)\mathbf{s}_{k-1}^L), \quad n = 1, \cdots, N, \tag{10}$$

followed by updating the leak locations by solving the one-dimensional optimization problem

$$x_k^{L_n} = \arg\max_{x^{L_n}} \hat{\mathbf{c}}_{nk}^H \frac{\mathbf{G}_n^H(x^{L_n})\mathbf{G}_n(x^{L_n})}{\mathbf{G}_n^H(x^{L_n})\mathbf{G}_n(x^{L_n})}\hat{\mathbf{c}}_{nk}, \quad n = 1, \cdots, N, \tag{11}$$

and updating the leak sizes via

$$s_k^{L_n} = \frac{\mathbf{G}_n^H(x_k^{L_n})\hat{\mathbf{c}}_{nk}}{\mathbf{G}_n^H(x_k^{L_n})\mathbf{G}_n(x_k^{L_n})}, \quad n = 1, \cdots, N. \tag{12}$$

The iteration stops when the relative increase of the observed data log-likelihood (7) is less than a given threshold κ:

$$\left|\frac{\log L(\mathbf{x}_k^L, \mathbf{s}_k^L|\Delta\mathbf{h}) - \log L(\mathbf{x}_{k-1}^L, \mathbf{s}_{k-1}^L|\Delta\mathbf{h})}{\log L(\mathbf{x}_{k-1}^L, \mathbf{s}_{k-1}^L|\Delta\mathbf{h})}\right| < \kappa. \tag{13}$$

After repeating the above procedure with different possible N, the number of leaks is estimated by minimizing the AIC with respect to N [36,41]:

$$\mathrm{AIC}(N) = 2NMJ - \log L\left(N, \hat{\mathbf{x}}_{(N)}^L, \hat{\mathbf{s}}_{(N)}^L|\Delta\mathbf{h}\right). \tag{14}$$

In this equation, $\hat{\mathbf{x}}_{(N)}^L$ and $\hat{\mathbf{s}}_{(N)}^L$ stand for the estimates of leak locations and sizes with N assumed leaks.

Finally, the whole procedure for estimating multiple leaks (locations, sizes, and leak number) is summarized in Algorithm 1.

Algorithm 1: Estimation of multiple leaks in a viscoelastic pipe

Select J frequencies $\omega_1, \cdots, \omega_J$.
Compute a_{ve} from Eq. (6) for the selected frequencies, where the coefficients N_{kv}, J_i and τ_i $(i = 1, \cdots, N_{kv})$ in the generalized K-V model are obtained from a previous intact pipe transient test.
Estimate the boundary condition $\hat{q}(x^U, \omega_j)$ from Eq. (4) using the pressure head measurements $h(x_0, \omega_j)$ at x_0 for the selected frequencies.
Calculate $h^{NL}(\omega_j, x_m)$ via Eq. (2) and use the head differences $\Delta\mathbf{h}$ as the data, which includes pressure head difference from the J frequencies and M sensors $(x_1, \cdots, x_M)$.
For $N = 0$, compute AIC(0) via Eq. (14).
repeat
  $N = N + 1$.
  if $N = 1$ or $N = 2$ **then**
    Plot Eq. (8) and retain its maximum as $\hat{\mathbf{x}}^L$.
    Obtain $\hat{\mathbf{s}}^L$ from Eq. (9).
    Compute AIC(N) via Eq. (14).
  else
    For $k = 0$, pick starting values $\mathbf{x}_0^L = \left(x_0^{L_1}, \cdots, x_0^{L_N}\right)^\top$ and $\mathbf{s}_0^L = \left(s_0^{L_1}, \cdots, s_0^{L_N}\right)^\top$ for the initial model parameters.
    For $k \geqslant 1$:
    repeat
      estimate the latent leak contribution $\hat{\mathbf{c}}_{nk}$, $n = 1, \cdots, N$, by Eq. (10).
      update the leak location $x_k^{L_n}$, $n = 1, \cdots, N$, by Eq. (11).
      update the leak size $s_k^{L_n}$, $n = 1, \cdots, N$, by Eq. (12).
    until the relative increase of the observed data log-likelihood is less than a given threshold κ, i.e., Eq. (13) holds.
    Let $\hat{\mathbf{x}}_{(N)}^L = \left(x_k^{L_1}, \cdots, x_k^{L_N}\right)^\top$ and $\hat{\mathbf{s}}_{(N)}^L = \left(s_k^{L_1}, \cdots, s_k^{L_N}\right)^\top$.
    Compute AIC(N) via Eq. (14).
  end if
until AIC(N) > AIC($N - 1$).
Retain $N - 1$ as the estimate of leak number, $\hat{\mathbf{x}}_{(N-1)}^L$ and $\hat{\mathbf{s}}_{(N-1)}^L$ as the final estimates of leak locations and sizes.

4. Experimental results

In this section, the experimental results of multi-leak estimation are introduced. The cases of two leaks and three leaks are respectively considered.

4.1. Experimental setup

The setup of the pipe system in the Water Resources Research Laboratory at the Hong Kong University of Science and Technology is shown in Fig. 2. The pipe wall material is HDPE, the pipe length is $l = 144$ m, and the internal diameter of cross-section is $d = 0.0792$ m. A pump is connected to the upstream of the pipe to move the water. The pre-transient pressure head and flow discharge are respectively 45.4 m and 5×10^{-4} m^3/s at the upstream end of the pipe, when no leak is present in the pipe. A valve is set at the downstream of the pipe to generate transient waves where the duration time of valve closure is around 0.05 s. Pressure head signals are measured at $x_0 = 36.92$ m, $x_1 = 141.43$ m and $x_2 = 122.25$ m by UNIK 5000 transducer connected to a National Instruments data logger (NI 9030). The sampling frequency is 1000 Hz. Three possible leaks are simulated at $x^{L_1} = 45.58$ m, $x^{L_2} = 69.31$ m and $x^{L_3} = 100.23$ m, as shown in Fig. 3. The coefficients in the generalized K-V model are calibrated using transient tests but with no leak [58]. The truncated order is $N_{kv} = 5$ and the corresponding coefficients J_j and $\tau_j, j = 1, \cdots, 5$, are obtained and shown in Table 1. Note that these coefficients are crucial for the accuracy of the proposed leakage detection method, as has been indicated in [51] for single leak case.

In the following two subsections, the experimental results of estimating two leaks (x^{L_1} and x^{L_2}) and three leaks (x^{L_1}, x^{L_2} and x^{L_3}) are introduced, respectively.

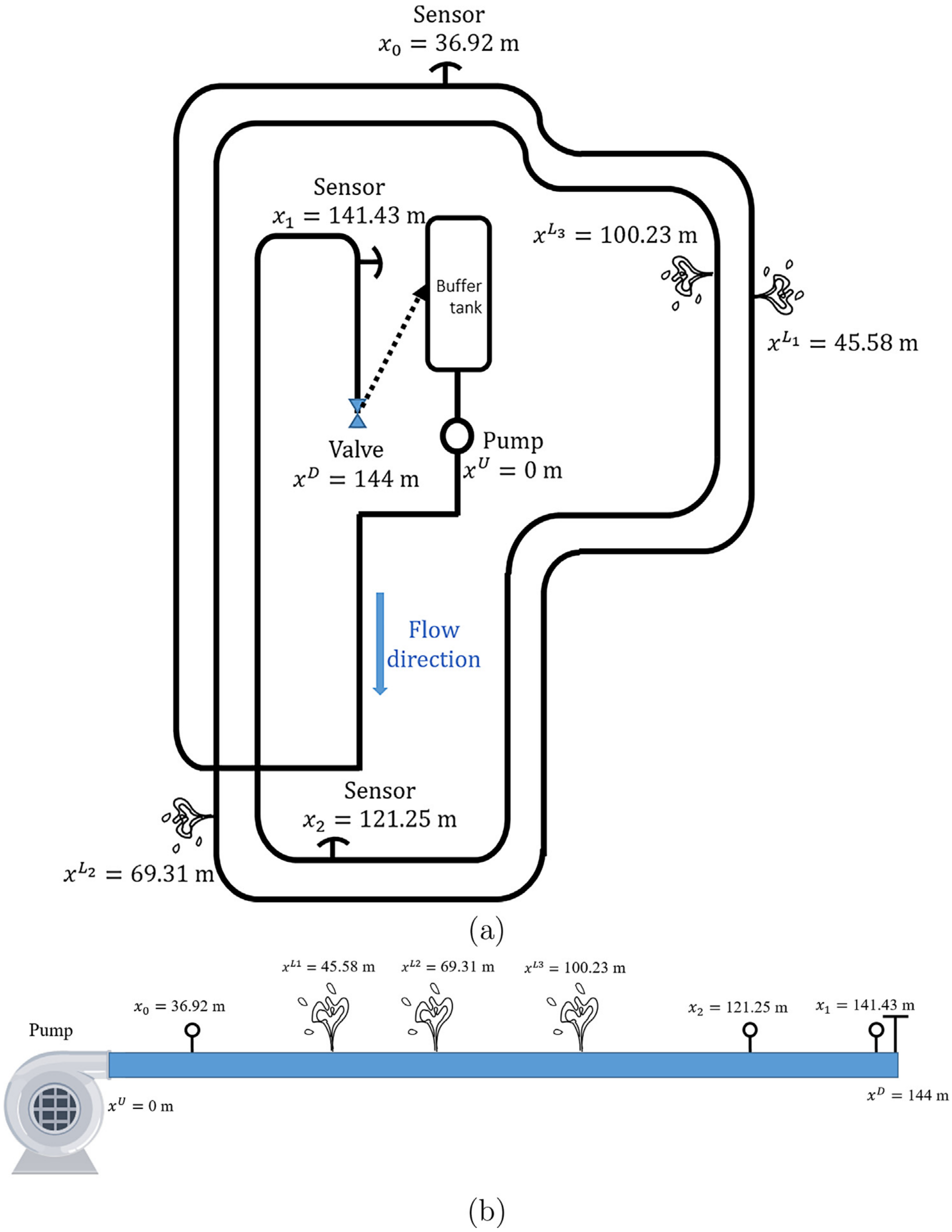

Fig. 2. Setup of the pipeline system in the Water Resources Research Laboratory at the Hong Kong University of Science and Technology.

4.2. Identification of two leaks

Here, estimation of two leaks located at $x^{L_1} = 45.58$ m and $x^{L_2} = 69.31$ m is considered. Fig. 4 (a) shows the measured time signal at three sensors at $x_0 = 36.92$ m, $x_1 = 141.43$ m, and $x_2 = 121.25$ m. Fig. 4 (b) plots FRF (cf. [51,59] for the derivation of FRF from time signal) with respect to angular frequency normalized by the fundamental angular frequency. It can seen from Fig. 4 that the measured signals include much random noise, which is partially due to the pump. In this section, all the available frequencies in $[\omega_{th}, 17\omega_{th}]$ are used for leakage estimation; here, the maximum used frequency is $17\omega_{th}$ because after this value the FRF in Fig. 4 (b) is noise dominated.

The viscoelastic wave speed is computed by inserting the K-V model coefficients in Table 1 into Eq. (6); its real and imaginary parts versus frequency are plotted in Fig. 5 (a). On the other hand, the wave speed can be estimated via travel time of wave from the measured pressure signal in Fig. 4 (a), as shown in Fig. 5 (b). The wave speed can be estimated by wave travel from x_1 to x_2 in the first half period, which is essentially the elastic wave speed since the viscoelastic effect (retarded strain)

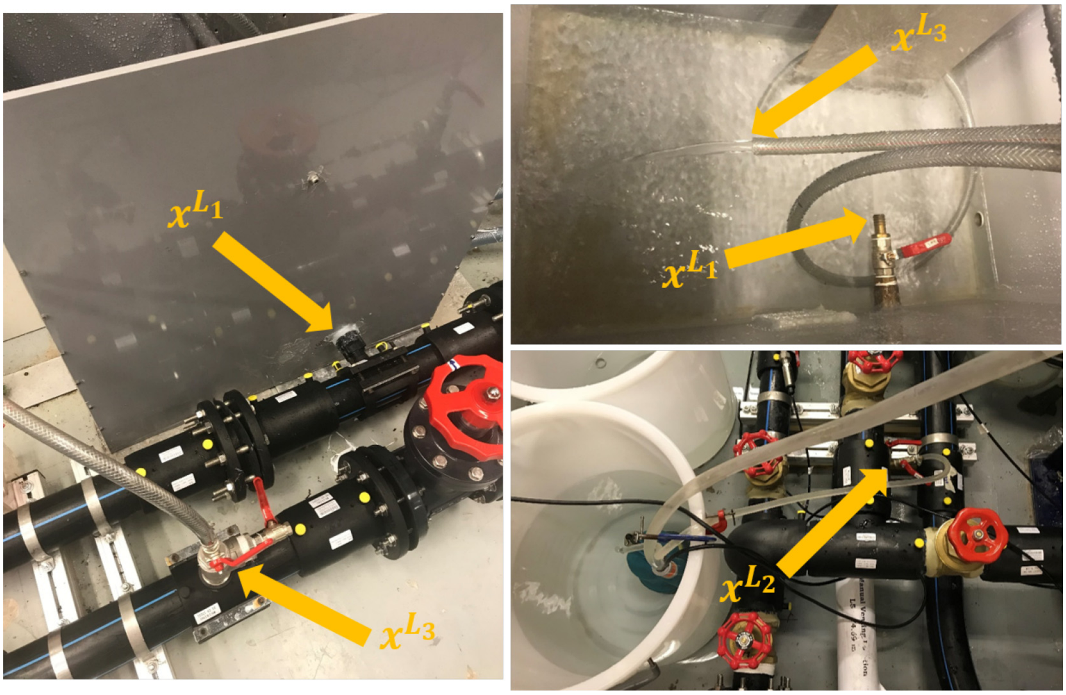

Fig. 3. Photos of the three leaks in the pipeline system at $x^{L_1} = 45.58$ m, $x^{L_2} = 69.31$ m and $x^{L_3} = 100.23$ m.

Table 1
Coefficients in the generalized K-V model.

$\nu = 0.46$	$\kappa = 2.1 \times 10^9$ Pa	$\rho = 10^3$ kg/m^3
$e = 5.4 \times 10^{-3}$ m	$J_0 = 1.5 \times 10^{-9}$ Pa^{-1}	$J_1 = 7.3 \times 10^{-11}$ Pa^{-1}
$\tau_1 = 0.05$ s	$J_2 = 1.7 \times 10^{-10}$ Pa^{-1}	$\tau_2 = 0.5$ s
$J_3 = 6.4 \times 10^{-11}$ Pa^{-1}	$\tau_3 = 1.5$ s	$J_4 = 5.7 \times 10^{-12}$ Pa^{-1}
$\tau_4 = 5$ s	$J_5 = 8.4 \times 10^{-12}$ Pa^{-1}	$\tau_5 = 10$ s

has few influence at this early time, as $\hat{a}_e = 367$ m/s. The wave speed can also be estimated by wave travel time using latter periods; Fig. 5 (b) shows the wave speed computed from wave travel times in the first, second, third and fourth periods (using the signal recorded by x_1), being 311 m/s, 285 m/s, 264 m/s and 248 m/s respectively, which approaches to the computed viscoelastic wave speed in Fig. 5 (a). This is because the viscoelastic effect (retarded strain) plays a more important role as the transient wave travels longer time. Since the leakage estimation method proposed in this paper uses many periods of time signals, considering the pipe wall viscoelasticity via $\hat{a}_{ve}$ in Eq. (6) implies a more accurate model and, therefore, a more accurate leakage estimation result can be expected.

The pressure head measurement from $x_0 = 36.92$ m is used to estimate $q(x^U)$ via Eq. (4) while measurements from $x_1 = 141.43$ m and $x_2 = 121.25$ m are used to form $\Delta\mathbf{h}$, i.e., $M = 2$. Fig. 6 (a) plots Eq. (8) for assumed leak number $N = 1$, where the vertical dash lines and crosses in the horizontal axis represent the actual leak locations and sensor locations, respectively. This figure shows that the plot for 1D search (this method is also known as MFP in [32,51]) has three main peaks: two of them correspond to the two actual leaks and another peak is fictitious. From the perspective of parameter estimation, only the maximum point is retained as the estimate of single leak. Fig. 6 (b) plots Eq. (8) with assumed leak number $N = 2$, where the cross represents actual leak locations. In this case where the assumed leak number equals to the actual leak number, the proposed method can accurately localize the two leaks: the estimates of leak locations are 44.42 m and 69.42 m while their actual values are 45.58 m and 69.31 m. When the assumed leak number $N \geqslant 3$, IB is used to estimate the leaks. The initial locations of the leaks in IB are selected from the local maxima in Fig. 6 (a), for example when $N = 3$ the three highest local maxima in Fig. 6 (a) are selected, while the initial leak sizes are all set to be 0. The threshold κ to stop the iteration of

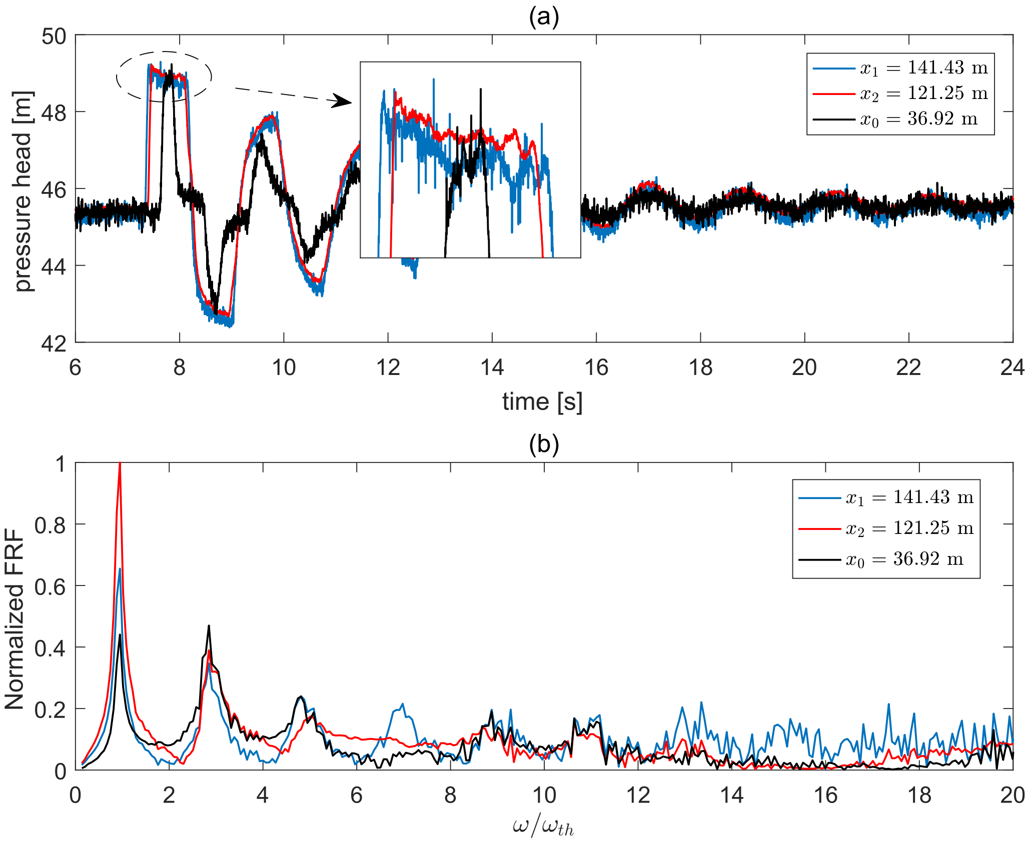

Fig. 4. Pressure head measurements in the time domain and in the frequency domain (FRF). The measurement locations are $x_0 = 36.92$ m, $x_1 = 141.43$ m, and $x_2 = 121.25$ m. The pipe has two leak at $x^{L_1} = 45.58$ m and $x^{L_2} = 69.31$ m.

the IB algorithm in Eq. (13) is set to be $\kappa = 10^{-4}$. Fig. 6 (c-f) shows the leak estimation results (plot of locations and sizes) for $N = 1, 2, 3, 4$, where the dash lines and crosses stand for actual leak locations and sensor locations, respectively. When $N = 3$, two estimates of leaks are close to the actual leaks; another estimated leak locates outside the range of pipe with a small leak size estimate and, thus, can be neglected. When $N = 4$, two estimates approximately reconstruct the leak at 69.42 m, but a fictitious leak appears in the result. Note that here the leak size estimates are not emphasized because, in practice, the estimation accuracy of leak size is not so important as the leak location. This is due to the fact the excavation cost for repairing leaks is decided by the estimation accuracy of leak location, although, generally speaking, the actual leak size affects the leak estimation accuracy. As a matter of fact, the sizes of both leaks are computed from steady-state flow rate measurement prior to the transient test (three ultrasonic flow meters are set to measure upstream and downstream flow rates of each leak), being approximately $s^{L_1} = s^{L_2} = 3 \times 10^{-5}$ m^2. It can be found in Fig. 6 (c-f) that the leak size is overestimated (about 1–1.5$\times 10^{-4}$ m^2) due to the presence of noise and modeling uncertainties.

The results in Fig. 6 show that $N = 1, 2, 3$ and 4 are all possible leak number solutions. The important practical question is how one selects the correct solution amongst this set. This is decided by the likelihood function and AIC. Their values versus assumed leak number N are shown in Fig. 7. Here, the noise standard deviation σ is estimated from prior multiple transient tests. It is clear that when N is greater than the actual leak number 2, the likelihood function increases but only slightly. In fact, more assumed leaks (or free parameters) fit the noise or uncertainties, instead of the desired signal, via ML. AIC essentially gives penalties for high leak number to avoid over-fitting and thus accurately decide the leak number, i.e., $\widehat{N} = 2$. Therefore, the results in Fig. 6 (b) and (d) are retained as the final estimate of leaks. This example shows that the AIC is able to decide the number of leaks in a pipe system.

4.3. Identification of three leaks

In this section, identification of three leaks is studied; all the three leaks in Fig. 3 are open. The pressure head measurements from the three hydrophones at $x_0 = 36.92$ m, $x_1 = 141.43$ m and $x_2 = 121.25$ m are shown in Fig. 8. The same proce-

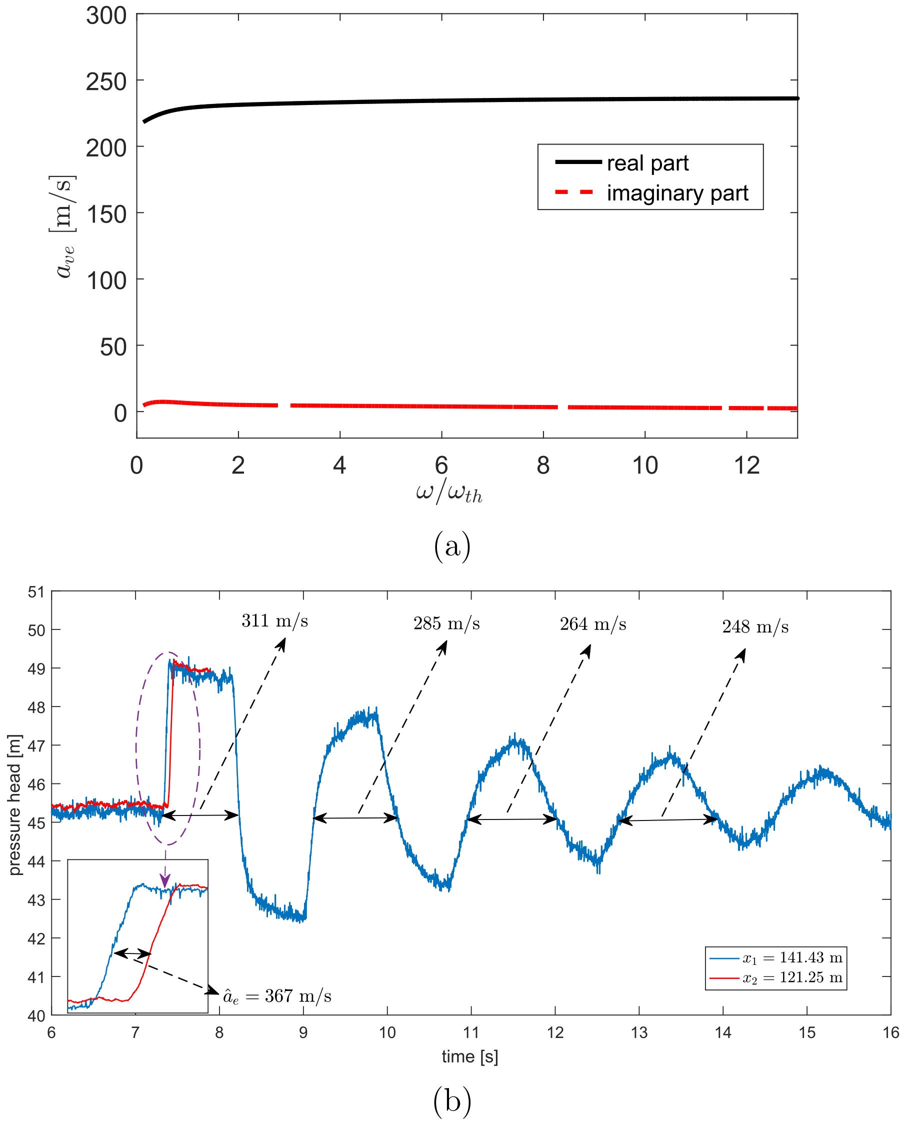

Fig. 5. (a): viscoelastic wave speed a_{ve} computed from Eq. (6); (b) wave speed estimated via wave travel time from the measured pressure signal.

dure with same selected frequencies and K-V model coefficients as the two-leak example is used to estimate leaks. Fig. 9 (a) plots Eq. (8) for assumed leak number $N = 1$. Its maximum is very close to the leak $x^{L_1} = 45.58$ m and retained as the output which results in Fig. 9 (b). Unlike the results in Section 4.2, however, the other two leaks cannot be identified from the 1D search in Fig. 9 (a). Note that as indicated in [32,60], the 1D search method for multiple leaks depends on the locations of the leaks and more leaks present in the pipe significantly increase the complexity of the leakage detection problem. Fig. 9 (c-f) shows the leakage estimation results with $N = 2, 3, 4, 5$; again, when $N = 2$ the 2D exhaustive search of leak locations via Eq. (8) is used, while when $N \geqslant 3$ the results are obtained from IB. It is clear that with the model of two leaks ($N = 2$), two of the three actual leaks are found. When the assumed and actual leak numbers are equal, i.e., $N = 3$, all the three leaks are localized. As N further increases, the ML scheme tends to use free parameters of two leaks to approximate one actual leak and ghost leak may appear. This phenomenon has also been found in the numerical results in [36]: more assumed leak number implies a more complicated inverse problem such that the algorithm more easily stops at local maxima. However, as is shown in Fig. 10 (left), more assumed leaks do not significantly increase the likelihood function, and thus AIC decides the leak number $\widehat{N} = 3$ (Fig. 10 (right)). Therefore, Fig. 9 (d) is retained as the final leakage localization result. Again, this example shows that the AIC technique is able to determine the number of leaks present in the pipe.

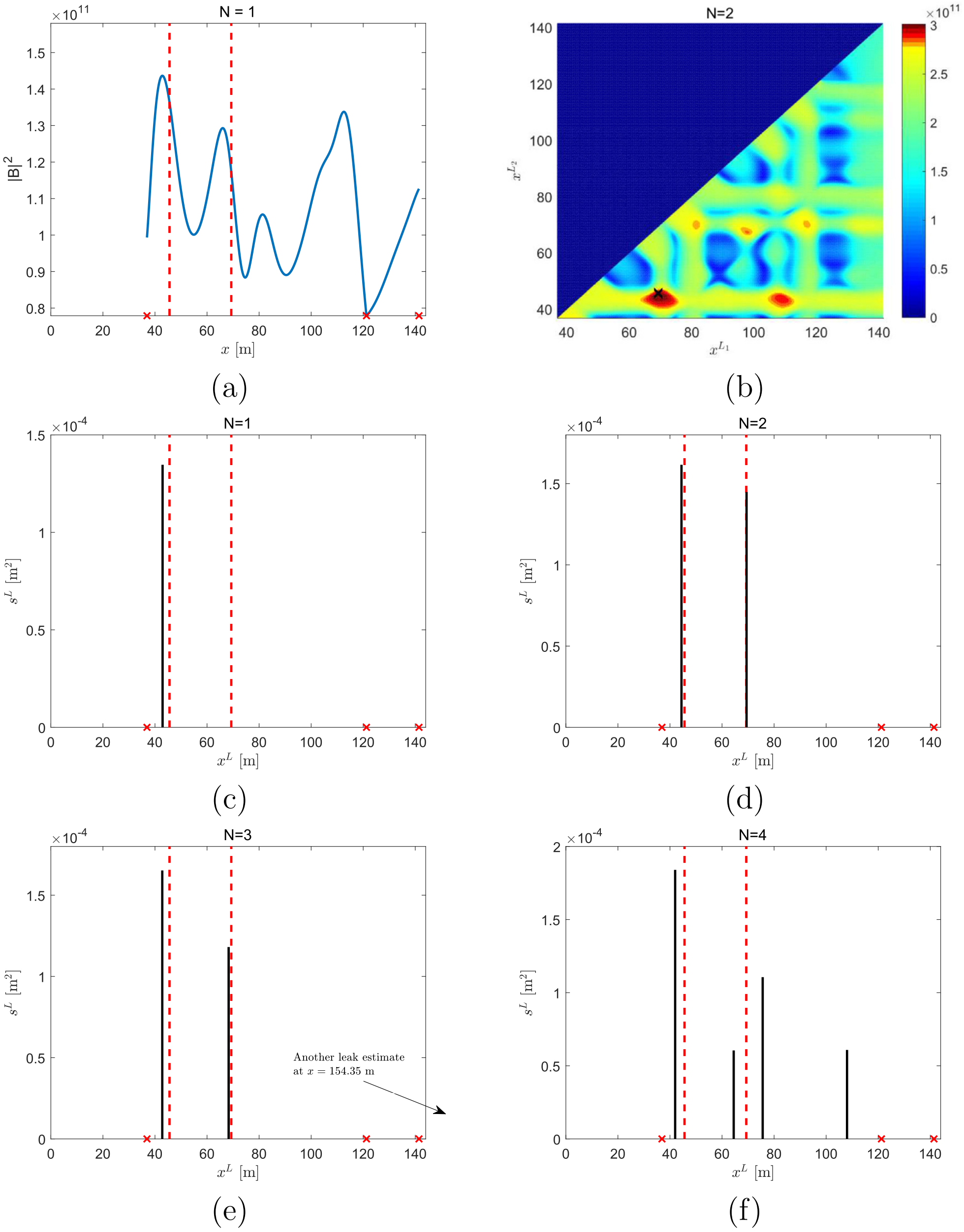

Fig. 6. Estimation of two leaks at $x^{L_1} = 45.58$ m and $x^{L_2} = 69.31$ m. (a) Plot of Eq. (8) for assumed leak number $N = 1$, where the dash lines and crosses stand for actual leak locations and sensor locations; (b) Plot of Eq. (8) for assumed leak number $N = 2$, where the cross represents actual leak locations; (c-f) leak estimation results (plot of locations and sizes) for $N = 1, 2, 3, 4$, where the dash lines and crosses stand for actual leak locations and sensor locations.

5. Conclusion

Following Part I and Part II of the series of papers which introduce the theoretical and numerical results for identification of multiple leaks, the present research verifies the proposed methodologies via experimental results. Data of transient test are collected from a recently-built pipe system in the Water Resources Research Laboratory at the Hong Kong University of Science and Technology. Since the pipe wall material is high-density polyethylene (HDPE), the previous transient model for elastic pipes is modified to quantify the effect of pipe wall viscoelasticity via the Kelvin-Voigt model. Experimental results with two and three leaks are shown. In both cases, the proposed multi-leak identification scheme is able to localize the leaks and decide the number of leaks accurately.

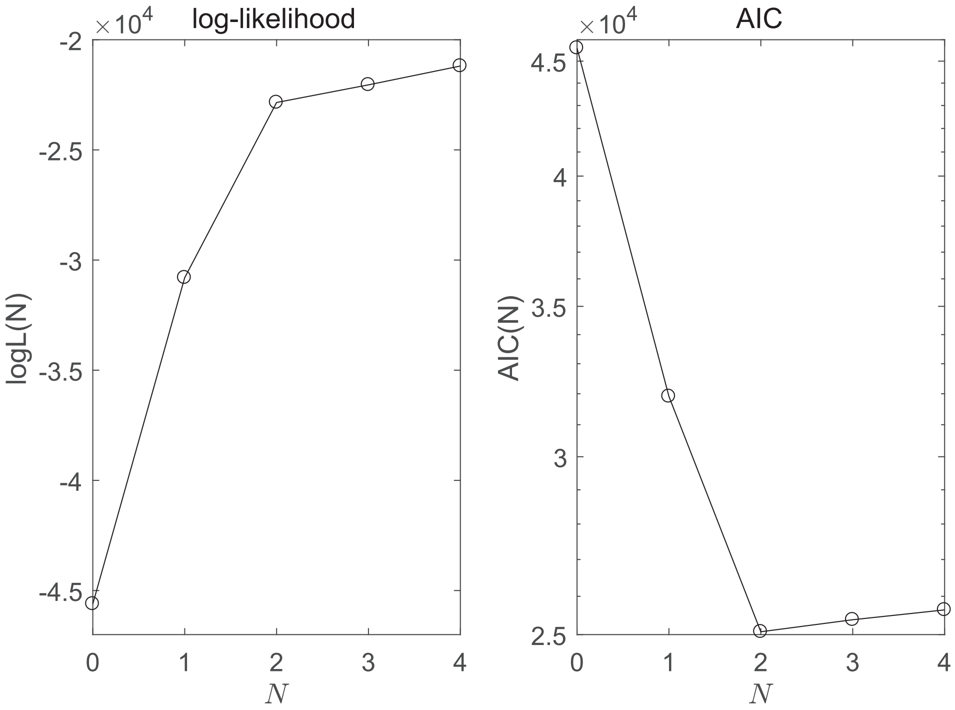

Fig. 7. Log-likelihood (left) and AIC (right) as a function of assumed leak number N. The actual leak number is 2 ($x^{L_1} = 45.58$ m and $x^{L_2} = 69.31$ m).

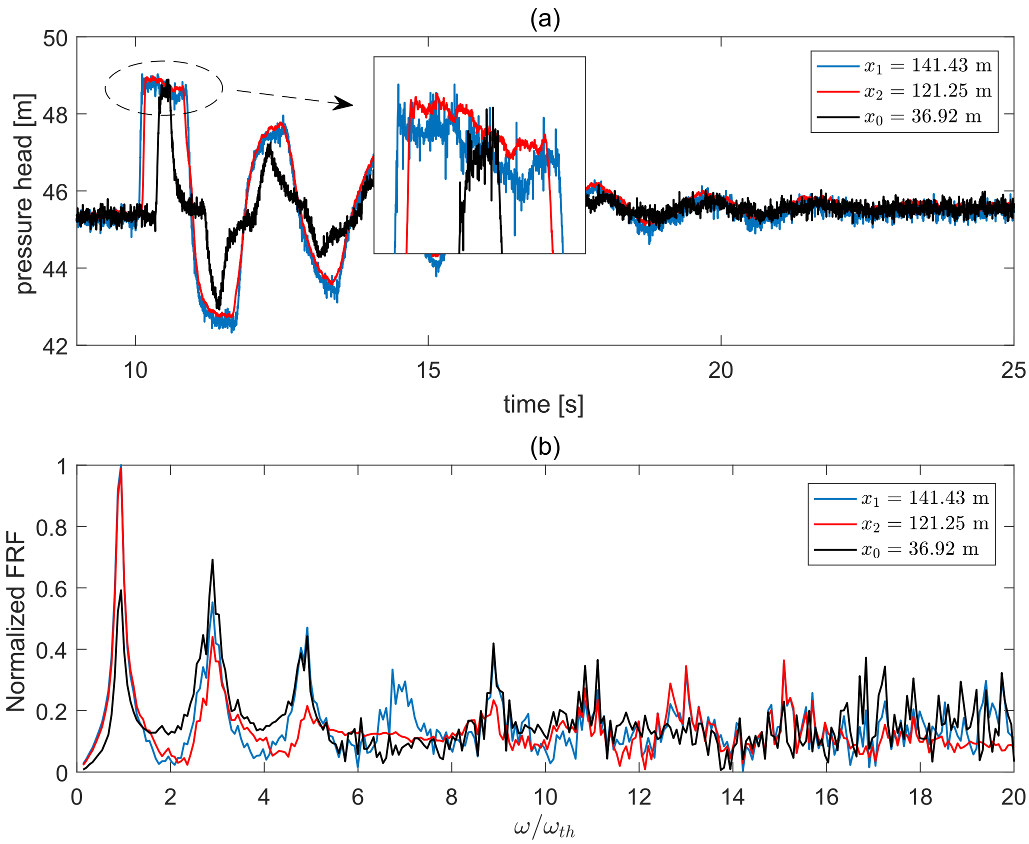

Fig. 8. Pressure head measurements in the time domain and in the frequency domain (FRF). The measurement locations are $x_0 = 36.92$ m, $x_1 = 141.43$ m, and $x_2 = 121.25$ m. The pipe has two leak at $x^{L_1} = 45.58$ m, $x^{L_2} = 69.31$ m and $x^{L_3} = 100.23$ m.

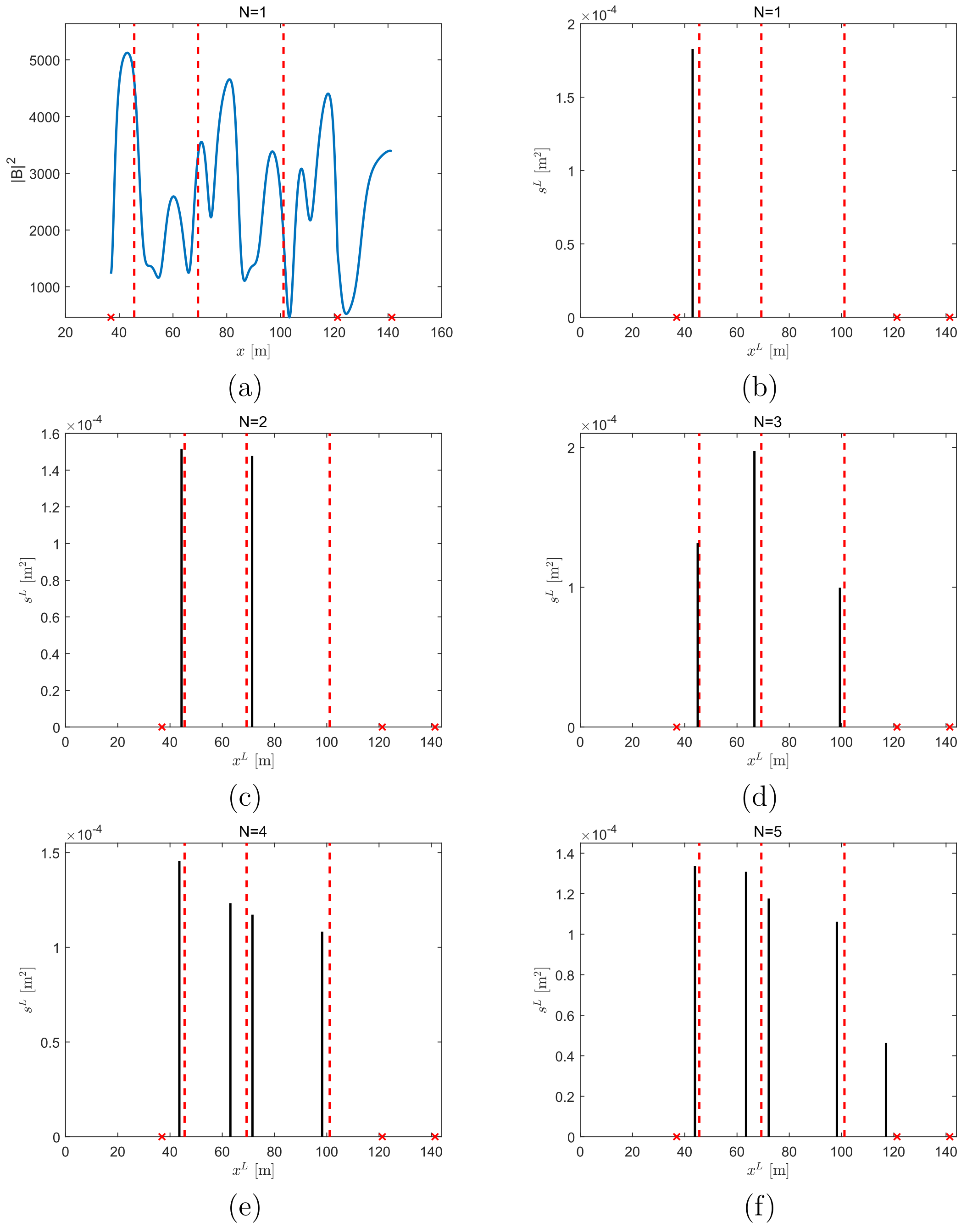

Fig. 9. Estimation of three leaks at $x^{L_1} = 45.58$ m, $x^{L_2} = 69.31$ m and $x^{L_3} = 100.23$ m. (a) Plot of Eq. (8) for assumed leak number $N = 1$; (b-f) leak estimation results (plot of locations and sizes) for $N = 1, 2, 3, 4, 5$. The dash lines and crosses stand for actual leak locations and sensor locations.

The accuracy of the transient wave model, particularly the viscoelastic coefficients in the model, is crucial for the proposed leakage detection method. The experiments in this paper are conducted in the laboratory and these coefficients are well-calibrated via transient data from a leak-free test. In real urban water supply systems, however, these coefficients depend on the change of surrounding environment including temperature and humidity. More importantly, transient test data without leak may not be available, particularly for aging pipe systems. Therefore, sensitivity of the proposed method with uncertain model parameters would be important and an inverse method that can further quantify the influence of these modeling uncertainties would be interesting.

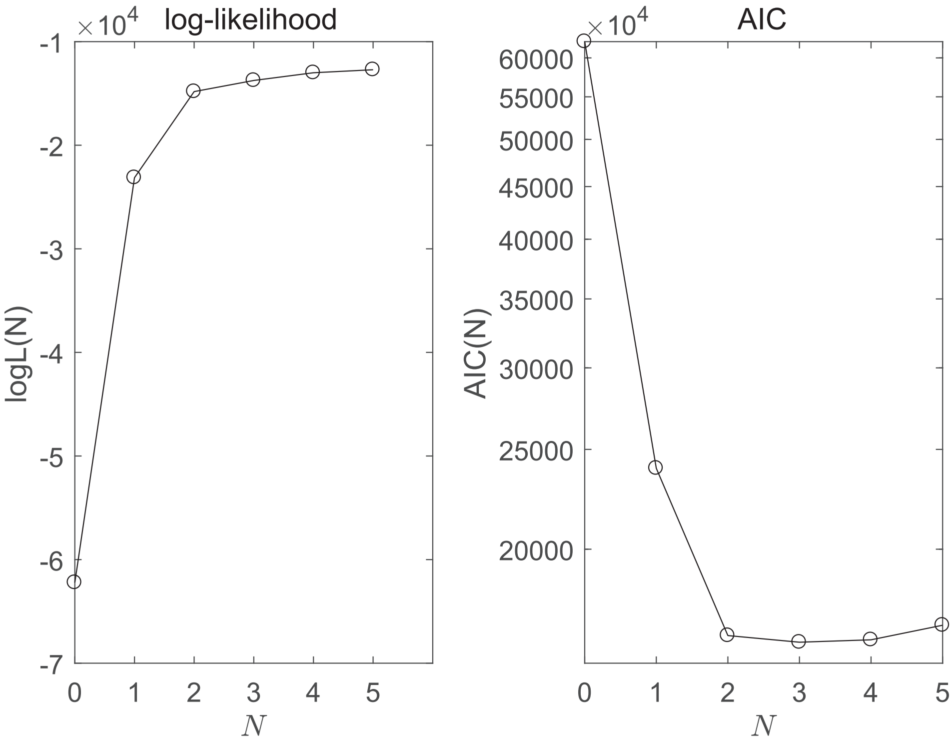

Fig. 10. Log-likelihood (left) and AIC (right) as a function of assumed leak number N. The actual leak number is 3 ($x^{L_1} = 45.58$ m, $x^{L_2} = 69.31$ m and $x^{L_3} = 100.23$ m).

Acknowledgements

This work has been supported by research grants from the Research Grant Council of the Hong Kong SAR, China (Project No.: T21-602/15R) and from Chinese Estates Professorship in Engineering (No.: R8031). The authors would like to thank Duncan A. McInnis, Asgar Ahadpour Dodaran, Man Yue Lam, Moez Louati, and Muhammad Waqar for their helps on the experiments at HKUST and two anonymous reviewers for their valuable comments and suggestions, which largely improved this paper.

References

[1] A.F. Colombo, P. Lee, B.W. Karney, A selective literature review of transient-based leak detection methods, J. Hydro-Environ. Res. 2 (4) (2009) 212–227.
[2] J.A. Liggett, L.-C. Chen, Inverse transient analysis in pipe networks, J. Hydraul. Eng. 120 (8) (1994) 934–955.
[3] B. Brunone, Transient test-based technique for leak detection in outfall pipes, J. Water Resour. Planning Manage. 125 (5) (1999) 302–306.
[4] J.P. Vítkovskỳ, A.R. Simpson, M.F. Lambert, Leak detection and calibration using transients and genetic algorithms, J. Water Resour. Planning Manage. 126 (4) (2000) 262–265.
[5] W. Mpesha, S.L. Gassman, M.H. Chaudhry, Leak detection in pipes by frequency response method, J. Hydraul. Eng. 127 (2) (2001) 134–147.
[6] X.-J. Wang, M.F. Lambert, A.R. Simpson, J.A. Liggett, J.P. Vítkovskỳ, Leak detection in pipelines using the damping of fluid transients, J. Hydraul. Eng. 128 (7) (2002) 697–711.
[7] P.J. Lee, J.P. Vitkovsky, M.F. Lambert, A.R. Simpson, J.A. Liggett, Frequency response coding for the location of leaks in single pipeline systems, in: The Int. Conference on Pumps, Electromechanical Devices and Systems Applied to Urban Water Management, IAHR and IHRA, Valencia, Spain, 2003.
[8] P.J. Lee, J.P. Vítkovskỳ, M.F. Lambert, A.R. Simpson, J.A. Liggett, Frequency domain analysis for detecting pipeline leaks, J. Hydraul. Eng. 131 (7) (2005) 596–604.
[9] P.J. Lee, J.P. Vítkovskỳ, M.F. Lambert, A.R. Simpson, J.A. Liggett, Leak location using the pattern of the frequency response diagram in pipelines: a numerical study, J. Sound Vib. 284 (3) (2005) 1051–1073.
[10] P.J. Lee, M.F. Lambert, A.R. Simpson, J.P. Vítkovskỳ, J. Liggett, Experimental verification of the frequency response method for pipeline leak detection, J. Hydraul. Res. 44 (5) (2006) 693–707.
[11] H.-F. Duan, P.J. Lee, M.S. Ghidaoui, Y.-K. Tung, Essential system response information for transient-based leak detection methods, J. Hydraul. Res. 48 (5) (2010) 650–657.
[12] H.-F. Duan, P.J. Lee, M.S. Ghidaoui, Y.-K. Tung, Leak detection in complex series pipelines by using the system frequency response method, J. Hydraul. Res. 49 (2) (2011) 213–221.
[13] H.-F. Duan, P.J. Lee, M.S. Ghidaoui, Y.-K. Tung, System response function-based leak detection in viscoelastic pipelines, J. Hydraul. Eng. 138 (2) (2011) 143–153.
[14] W. Nixon, M.S. Ghidaoui, Numerical sensitivity study of unsteady friction in simple systems with external flows, J. Hydraul. Eng. 133 (7) (2007) 736–749.

[15] M.F. Ghazali, S.B.M. Beck, J.D. Shucksmith, J.B. Boxall, W.J. Staszewski, Comparative study of instantaneous frequency based methods for leak detection in pipeline networks, Mech. Syst. Signal Processing 29 (2012) 187–200.
[16] A.C. Zecchin, L.B. White, M.F. Lambert, A.R. Simpson, Parameter identification of fluid line networks by frequency-domain maximum likelihood estimation, Mech. Syst. Signal Processing 37 (1) (2013) 370–387.
[17] S. Meniconi, B. Brunone, M. Ferrante, C. Capponi, C.A. Carrettini, C. Chiesa, D. Segalini, E.A. Lanfranchi, Anomaly pre-localization in distribution–transmission mains by pump trip: preliminary field tests in the milan pipe system, J. Hydroinf. 17 (3) (2015) 377–389.
[18] S. Meniconi, B. Brunone, M. Ferrante, C. Massari, Potential of transient tests to diagnose real supply pipe systems: What can be done with a single extemporary test, J. Water Resour. Planning Manage. 137 (2) (2010) 238–241.
[19] B. Brunone, M. Ferrante, Detecting leaks in pressurised pipes by means of transients, J. Hydraul. Res. 39 (5) (2001) 539–547.
[20] D. Covas, H. Ramos, N. Graham, C. Maksimovic, Application of hydraulic transients for leak detection in water supply systems, Water Sci. Technol.: Water Supply 4 (5–6) (2005) 365–374.
[21] S.T.N. Nguyen, J. Gong, M.F. Lambert, A.C. Zecchin, A.R. Simpson, Least squares deconvolution for leak detection with a pseudo random binary sequence excitation, Mech. Syst. Signal Processing 99 (2018) 846–858.
[22] M. Ferrante, B. Brunone, S. Meniconi, Wavelets for the analysis of transient pressure signals for leak detection, J. Hydraul. Eng. 133 (11) (2007) 1274–1282.
[23] W. Nixon, M.S. Ghidaoui, A.A. Kolyshkin, Range of validity of the transient damping leakage detection method, J. Hydraul. Eng. 132 (9) (2006) 944–957.
[24] J.C. Liou, Pipeline leak detection by impulse response extraction, J. Fluids Eng. 120 (4) (1998) 833–838.
[25] M. Ferrante, B. Brunone, Pipe system diagnosis and leak detection by unsteady-state tests. 1. Harmonic analysis, Adv. Water Resour. 26 (1) (2003) 95–105.
[26] D. Covas, H. Ramos, A.B. De Almeida, Standing wave difference method for leak detection in pipeline systems, J. Hydraul. Eng. 131 (12) (2005) 1106–1116.
[27] J. Lin, X. Wang, M.S. Ghidaoui, Theoretical investigation of leak's impact on normal modes of a water-filled pipe: small to large leak impedance, J. Hydraul. Eng. 145 (6) (2019) 04019017.
[28] A.M. Sattar, M.H. Chaudhry, Leak detection in pipelines by frequency response method, J. Hydraul. Res. 46 (EI1) (2008) 138–151.
[29] M. Taghvaei, S.B.M. Beck, J.B. Boxall, Leak detection in pipes using induced water hammer pulses and cepstrum analysis, Int. J. COMADEM 13 (1) (2010) 19.
[30] M.L. Stephens, Transient Response Analysis for Fault Detection and Pipeline Wall Condition Assessment in Field Water Transmission and Distribution Pipelines and Networks PhD Thesis, University of Adelaide, 2008.
[31] D. Covas, H. Ramos, Case studies of leak detection and location in water pipe systems by inverse transient analysis, J. Water Resour. Planning Manage. 136 (2) (2010) 248–257.
[32] X. Wang, M.S. Ghidaoui, Pipeline leak detection using the matched-field processing method, J. Hydraul. Eng. 144 (6) (2018) 04018030.
[33] B. Zhou, A. Liu, X. Wang, Y. She, V. Lau, Compressive sensing-based multiple-leak identification for smart water supply systems, IEEE Internet Things J. 5 (2) (2018) 1228–1241.
[34] A. Keramat, X. Wang, M. Louati, S. Meniconi, B. Brunone, M.S. Ghidaoui, Objective functions for inverse transient analysis based pipeline leakage detection: least square and matched-filter, J. Water Resour. Planning Manage. (2019), in press, 10.1061/(ASCE)WR.1943–5452.0001108.
[35] X. Wang, M.S. Ghidaoui, Identification of multiple leaks in pipeline: linearized model, maximum likelihood, and super-resolution localization, Mech. Syst. Signal Processing 107 (2018) 529–548.
[36] X. Wang, M.S. Ghidaoui, Identification of multiple leaks in pipeline II: iterative beamforming and leak number estimation, Mech. Syst. Signal Processing 119 (2019) 346–362.
[37] M. Feder, E. Weinstein, Parameter estimation of superimposed signals using the EM algorithm, IEEE Trans. Acoust., Speech Signal Processing 36 (4) (1988) 477–489.
[38] X. Wang, B. Quost, J.-D. Chazot, J. Antoni, Iterative beamforming for identification of multiple broadband sound sources, J. Sound Vib. 365 (2016) 260–275.
[39] X. Wang, B. Quost, J.-D. Chazot, J. Antoni, Estimation of multiple sound sources with data and model uncertainties using the EM and evidential EM algorithms, Mech. Syst. Signal Processing 66–67 (2016) 159–177.
[40] X. Wang, S. Khazaie, L. Margheri, P. Sagaut, Shallow water sound source localization using the iterative beamforming method in an image framework, J. Sound Vib. 395 (2017) 354–370.
[41] H. Akaike, A new look at the statistical identification model, IEEE Trans. Autom. Control 19 (1974) 716–723.
[42] G. Schwarz, Estimating the dimension of a model, Ann. Stat. 6 (2) (1978) 461–464.
[43] P.G. Franke, Computation of unsteady pipe flow with respect to visco-elastic material properties, J. Hydraul. Res. 21 (5) (1983) 345–353.
[44] G. Pezzinga, P. Scandura, Unsteady flow in installations with polymeric additional pipe, J. Hydraul. Eng. 121 (11) (1995) 802–811.
[45] D. Covas, I. Stoianov, H. Ramos, N. Graham, C. Maksimovic, The dynamic effect of pipe-wall viscoelasticity in hydraulic transients. Part I–experimental analysis and creep characterization, J. Hydraul. Res. 42 (5) (2004) 517–532.
[46] D. Covas, I. Stoianov, J.F. Mano, H. Ramos, N. Graham, C. Maksimovic, The dynamic effect of pipe-wall viscoelasticity in hydraulic transients. Part ii–model development, calibration and verification, J. Hydraul. Res. 43 (1) (2005) 56–70.
[47] A. Keramat, A.S. Tijsseling, Q. Hou, A. Ahmadi, Fluid–structure interaction with pipe-wall viscoelasticity during water hammer, J. Fluids Struct. 28 (2012) 434–455.
[48] H.-F. Duan, M. Ghidaoui, P.J. Lee, Y.-K. Tung, Unsteady friction and visco-elasticity in pipe fluid transients, J. Hydraul. Res. 48 (3) (2010) 354–362.
[49] A.K. Soares, D.I.C. Covas, L. Fernanda, R. Reis, Leak detection by inverse transient analysis in an experimental pvc pipe system, J. Hydroinf. 13 (2) (2011) 153–166.
[50] S. Meniconi, B. Brunone, M. Ferrante, C. Massari, Numerical and experimental investigation of leaks in viscoelastic pressurized pipe flow, Drinking Water Eng. Sci. 6 (1) (2013) 11–16.
[51] X. Wang, J. Lin, A. Keramat, M.S. Ghidaoui, S. Meniconi, B. Brunone, Matched-field processing for leak localization in a viscoelastic pipe: an experimental study, Mech. Syst. Signal Process. 124 (2019) 459–478.
[52] A. Kashima, P.J. Lee, R. Nokes, Numerical errors in discharge measurements using the KDP method, J. Hydraul. Res. 50 (1) (2012) 98–104.
[53] A. Kashima, P.J. Lee, M.S. Ghidaoui, M. Davidson, Experimental verification of the kinetic differential pressure method for flow measurements, J. Hydraul. Res. 51 (6) (2013) 634–644.
[54] B. Brunone, S. Meniconi, C. Capponi, Numerical analysis of the transient pressure damping in a single polymeric pipe with a leak, Urban Water J. (2018) 1–9.
[55] S. Meniconi, B. Brunone, M. Ferrante, C. Massari, Energy dissipation and pressure decay during transients in viscoelastic pipes with an in-line valve, J. Fluids Struct. 45 (2014) 235–249.
[56] A.P. Dempster, N.M. Laird, D.B. Rubin, Maximum likelihood from incomplete data via the EM algorithm, J. R. Stat. Soc., Series B (Methodology) 39 (1) (1977) 1–38.
[57] J.C.F. Wu, On the convergence properties of the EM algorithm, Ann. Stat. 11 (1983) 95–103.
[58] G. Pezzinga, B. Brunone, S. Meniconi, Relevance of pipe period on Kelvin-Voigt viscoelastic parameters: 1D and 2D inverse transient analysis, J. Hydraul. Eng. 142 (12) (2016) 04016063.
[59] P.J. Lee, Using System Response Functions of Liquid Pipelines for Leak and Blockage Detection, The University of Adelaide, Adelaide AU, 2005, PhD Thesis.
[60] X. Wang, D.P. Palomar, L. Zhao, M.S. Ghidaoui, R.D. Murch, Spectral-based methods for pipeline leakage detection, J. Hydraul. Eng. 145 (3) (2019) 04018089.